

Does Substrate Rather Than Protein Provide the Catalyst for α -Proton Abstraction in Aldolase?

R. A. Periana, Rossana Motiu-DeGrood, Yvonne Chiang, and D. J. Hupe*

Contribution from the Department of Chemistry, University of Michigan
Ann Arbor, Michigan 48109. Received October 9, 1979

Abstract: Dihydroxyacetone sulfate (DHAS) forms an iminium ion with rabbit muscle aldolase as does the natural substrate dihydroxyacetone phosphate (DHAP), but DHAS does not undergo subsequent α -proton abstraction to form enamine, as has been shown by Grazi. We propose that the phosphate group of DHAP acts as the catalyst for α -proton abstraction by an intramolecular mechanism and that the sulfate is too weakly basic to accomplish the same function. In this study a model system is presented in which intramolecular proton abstraction does occur in the elimination of *p*-nitrophenol from 4-(4-nitrophenoxy)-2-ketobutyl phosphate (**3**) but does not occur for the corresponding sulfate **1**. The compound 2-keto-3-butenyl sulfate (**2**) acts as an essentially irreversible inhibitor of aldolase in a manner similar to that previously shown for the phosphate analogue **4**. The proposed mechanism for inactivation, reversible iminium ion formation followed by subsequent addition of an active-site thiol, requires no proton transfer. The fact that **2** and **4** both act as inhibitors is consistent with the intramolecular proton transfer mechanism. The reversible binding of **2** is much less favorable than that of **4**, which is analogous to the relative favorability for binding of DHAS and DHAP. The maximum rate of conversion of dissociable complex to inhibited enzyme (addition of thiol to iminium ion) is roughly equivalent for **2** and **4**. This means that the ability of the iminium ion to act as an electron sink is not impaired by a change from phosphate to sulfate, and the major change is in the ability of the α -proton abstracting base to perform its role, as is consistent with an intramolecular proton transfer mechanism. A mechanism is proposed for the aldolase reaction which integrates the intramolecular proton transfer with stereochemical features of the transformation, the presence of various functional groups at the active site, and the order with which substrates are bound to the enzyme.

Introduction

Aldolase, the enzyme responsible for cleavage of fructose 1,6-bisphosphate (F-1,6-P₂) into trioses, has been studied by many enzymologists because of the central role that it plays in cellular metabolism. This has resulted in evidence for the existence of a number of functional groups at the active site and speculation concerning their importance in the catalytic mechanism.¹ Some of the most important observations concerning imine-forming (class I) aldolases typified by rabbit muscle aldolase are shown in Scheme I. The iminium ion formed from the essential lysine amino group and dihydroxyacetone phosphate (DHAP) may undergo (a) reduction by borohydride,² (b) reaction with cyanide,³ (c) stereospecific α -proton exchange with solvent water,⁴ and (d) the aldol condensation reaction with glyceraldehyde 3-phosphate (G-3-P) and other aldehydes.¹

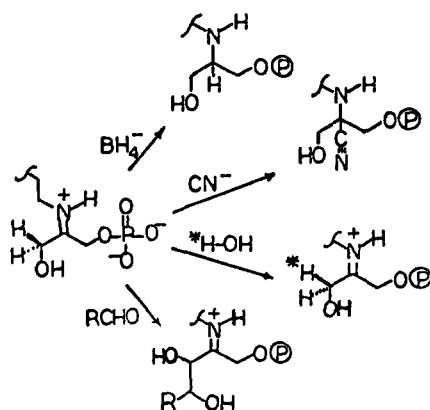
In an interesting study, Grazi has shown that the sulfur analogue, dihydroxyacetone sulfate (DHAS), exhibits somewhat different behavior.⁵ DHAS binds less well than does DHAP to form the iminium ion. Once formed, however, the iminium ion undergoes reduction with borohydride or reaction with cyanide just as did DHAP. The fact that these reactions exhibited different pH dependencies for DHAP and DHAS led to the suggestion that the reactivity of the iminium ion was

altered by the ionized group. It was also found that DHAS did not undergo proton transfer leading to exchange with solvent, nor did it undergo condensation to form an aldol product. Though iminium ion formation with DHAS does occur, subsequent α -proton abstraction does not. It is not clear whether the proton transfer is prevented because the change from phosphate to sulfate affects the reactivity of the iminium ion in acting as an electron sink or because this change alters the ability of the proton-abstracting base to perform its role.

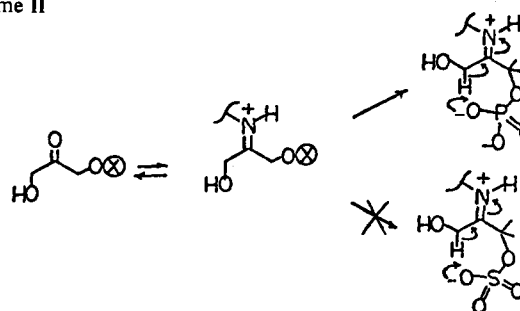
One logical explanation for this behavior is that the phosphate group on DHAP acts as the catalyst for proton abstraction from the iminium ion. As shown in Figure 1, we have previously demonstrated the ability of an α -ketophosphate to catalyze its own enolization via a seven-membered transition state.^{6,7} Aldolase, therefore, could be operating in a similar manner as shown in Scheme II. Both DHAP and DHAS may form the intermediate iminium ion, but only DHAP would carry out the subsequent proton transfer because the oxyanion on the sulfate would presumably be too weakly basic.

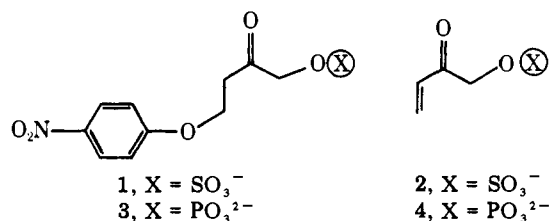
In this study we wanted to determine if changing from phosphate to sulfate in a model system would prevent intramolecular proton transfer from occurring. We also wished to find out if the change from phosphate to sulfate dramatically altered the reactivity of the iminium ion at the active site. Compound **1** was desired because the pH-rate profile for the conversion from **1** to **2** should show whether sulfate is capable of catalyzing the intramolecular proton abstraction. This would also generate **2**, which is the sulfate analogue of **4**, a potent active site directed covalent inhibitor of rabbit muscle aldolase.

Scheme I



Scheme II





Compound **4** has been shown to undergo a reversible binding followed by an essentially irreversible step leading to inactive enzyme.⁶ We have proposed that this behavior reflects reversible iminium ion formation followed by the addition of an active-site thiol as shown in Scheme III. This reaction is of interest in this study because it requires no proton transfer to carbon (and therefore **1** and **4** should show no difference if the intramolecular mechanism operates) and because $k_{\text{obsd}}^{\text{max}}$ would give a good indication of whether the change from phosphate to sulfate alters the reactivity of the iminium ion substantially.

We present below, therefore, syntheses of **1** and **2**, a study of the pH dependence of the conversion of **1** to **2**, and a study of the attempts to inhibit aldolase with **2**.

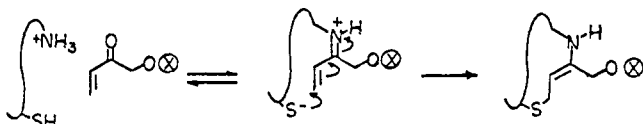
Experimental Section

4-(4-Nitrophenoxy)-2-keto-*n*-butyl Acetate (6). **5** (0.93 g, 3.9 mmol), prepared as previously described,⁶ was added to 10 mL of acetic acid. The mixture was heated to 70 °C and stirred for 0.5 h. During this time a spot due to **5** on TLC (R_f 0.2, silica gel, ether) disappeared as one for **6** (R_f 0.35) appeared. The excess acetic acid and any other volatile components were removed under reduced pressure. Two 10-mL portions of ether were added to the resulting solid and removed under reduced pressure. The tan solid thus obtained was recrystallized from ether, yielding 0.96 g (3.6 mmol, 93% yield) of **6**: mp 101–103 °C; IR (KBr) 1748, 1725 cm⁻¹; ¹H NMR (CDCl₃) δ 2.15 (s, 3 H), 2.96 (t, 2 H, $J = 7$ Hz), 4.34 (t, 2 H, $J = 7$ Hz), 6.97 (d, 2 H, $J = 10$ Hz), 8.04 (d, 2 H, $J = 10$ Hz); MS 267, M⁺.

4-(4-Nitrophenoxy)-2-ketobutanol Ethylene Ketal (7). To 0.90 g of **6** (3.4 mmol) was added 10 mL of ethylene glycol. The mixture was heated to 70 °C and stirred until the solid dissolved. *p*-Toluenesulfonic acid monohydrate (10 mg) was added, the temperature was adjusted to 60 °C, and the reaction mixture was stirred for 36 h. During this time a spot due to **7** (R_f 0.55, silica gel, ether) appeared. To the cooled reaction mixture 20 mL of 0.1 N NaOH solution was added. The resulting yellow solution was then extracted with 3 × 10 mL portions of ether. The combined ether extracts were washed with 3 × 10 mL portions of distilled water. The ether solution was dried over anhydrous sodium sulfate and the ether removed under reduced pressure. The white solid resulting was recrystallized from ether, yielding 0.82 g (3.0 mmol, 90% yield) of **7**: mp 72–74 °C; IR (KBr) 3480, 1596, 1180 cm⁻¹; ¹H NMR (CDCl₃ shaken with D₂O) δ 2.13 (t, 2 H, $J = 7$ Hz), 3.56 (s, 2 H), 4.00 (s, 4 H), 4.18 (t, 2 H, $J = 7$ Hz), 7.98 (d, 2 H, $J = 10$ Hz), 8.16 (d, 2 H, $J = 10$ Hz); MS (no molecular ion⁸) 238 (-CH₂OH).

4-(4-Nitrophenoxy)-2-keto-1-butanol (8). **7** (0.78 g, 29 mmol) was dissolved in 5 mL of acetonitrile and 5 mL of distilled water was added, along with 3 drops of concentrated hydrochloric acid. The mixture was shaken vigorously for 5 min and then extracted with 3 × 10 mL portions of ether. The combined ether extracts were washed with 3 × 5 mL portions of distilled water, and the resulting ether solution was dried over anhydrous sodium sulfate. The ether was removed under reduced pressure, and the resulting oil was recrystallized from chloroform to give 0.61 g of **8** (2.7 mmol, 95% yield): mp 160–170 °C dec; IR (KBr) 3420, 1710 cm⁻¹; ¹H NMR (CDCl₃) δ 2.93 (t, 2 H, $J = 7$ Hz), 2.98 (s, br, 1 H), 4.31 (s, 2 H), 4.38 (t, 2 H, $J = 7$ Hz), 6.87 (d, 2 H, $J = 9$ Hz), 8.10 (d, 2 H, $J = 9$ Hz); MS M⁺, 225, 194.

Scheme III



4-(4-Nitrophenoxy)-2-ketobutyl Sulfate Potassium Salt Monohydrate (1). A 0.55-g sample of **8** (2.5 mmol) was dissolved in 10 mL of dry dimethylformamide. The solution was cooled to 0 °C and 3 mL of 15% fuming H₂SO₄ was added with rapid stirring. The reaction mixture was kept at this temperature for 24 h. During this time, small aliquots dissolved in distilled water and extracted three times with ether showed increasing yellow color in pH buffer but none in pH 7 buffer. The resulting solution was then added slowly to 20 mL of cold distilled water. This mixture was then extracted with 5 × 10 mL portions of ether. The aqueous solution thus obtained was titrated with 0.1 N potassium hydroxide solution to pH 3. Using KOH to finish the titration invariably caused the conversion of **1** to **2** as indicated by the production of *p*-nitrophenol. Therefore, potassium β-naphthoate was added until the pH of the reaction mixture was between pH 4 and 5. The β-naphthoic acid thus produced was filtered off, and the solution was extracted with 2 × 15 mL portions of ether. Small aliquots of this solution did not instantly turn yellow when raised to pH 8 but rapidly turned yellow when the pH was raised to 10. The intensity of this absorption in diluted aliquots allowed the estimation of the conversion of **8** to **1**, which was approximately 60%.

Solutions of **1**, thus prepared, were separated from the excess potassium sulfate and any other impurities by chromatography on a Sephadex G-10 column (2.0 × 25 cm). In a typical separation, 20 mL of the solution was loaded onto the column and eluted with distilled water. The fractions between 55 and 70 mL showed an intense yellow color when aliquots were added to NaOH solution, but no color when added to pH 7 buffer. These fractions were combined, frozen, and concentrated by lyophilization. The concentrated solutions were rechromatographed and lyophilized to yield a white, fluffy solid. The material was dissolved in the minimum amount of distilled water and cooled to 5 °C, whereupon small white crystals formed and were filtered off. These were washed with cold distilled water and dried. These washings and the supernatant were concentrated by lyophilization, and the crystallization process was repeated. This crystalline material had an average molecular weight of 361 ± 2, measured by *p*-nitrophenol production,⁶ which is consistent with a monohydrate. This procedure gives a 40% yield (343 mg, 25% overall from **5**) of crystalline monohydrate: mp 138–140 °C; IR (KBr) 1741 cm⁻¹; ¹H NMR (Me₂SO-*d*₆) δ 3.11 (t, 2 H, $J = 6$ Hz), 4.35 (s, 2 H), 4.36 (t, 2 H, $J = 6$ Hz), 7.18 (d, 2 H, $J = 9$ Hz), 8.22 (d, 2 H, $J = 9$ Hz); MS 225.1 (-SO₃).

Anal. Calcd for C₁₀H₁₂O₉ NSK: C, 33.24; H, 3.35; N, 3.87; S, 8.87. Found: C, 34.20; H, 3.38; N, 4.05; S, 8.91.

Several attempts to obtain a more satisfactory elemental analysis were unsuccessful.

2-Keto-3-butenyl Sulfate (2). To 0.18 g of **1** (0.5 mmol) was added 1 mL of distilled water. The solution was placed in an ice bath and with rapid stirring 1 N sodium hydroxide solution was added in very small aliquots using a dial type pipet to maintain the pH at 10. When no more base was required to maintain the pH at 10, the pH of the reaction mixture was lowered with 1 N HCl to pH 8.5. The resulting solution was loaded onto a Sephadex G-10 column (2 × 15 cm) and eluted with distilled water. The fractions eluted between 11 and 15 mL showed the characteristic UV absorption spectra of an enone ($\lambda_{\text{max}} = 215$ nm and $\epsilon = 6.2 \times 10^3$). Some of this solution was lyophilized to yield a white, fluffy solid to which D₂O was added, in order to obtain the ¹H NMR spectra: (D₂O) δ 4.84 (s, 2 H), 6.05 (m, 1 H), 6.30 (m, 2 H).

The pH-rate profile for the conversion of **1** to **2** was obtained by measuring the rate of appearance of *p*-nitrophenoxide at various pH values. Tris buffer at low concentrations (<10⁻⁴ M) was used to maintain the pH, and extrapolation of four values of k_{obsd} to zero buffer concentration gave the values shown in Figure 1. The values of k_{obsd} at low pH were obtained by initial rates. The ionic strength was 1.0, maintained with KCl.

Rabbit muscle aldolase was purchased from Calbiochem and desalted on a prepacked Sephadex PD-10 column. The aldolase concentration was calculated using $\epsilon_{280}^{1\%} = 9.38$.⁹ Activity of aldolase in incubation mixtures was determined by adding 0.050 mL to 0.750 mL of an assay mixture obtained from Calbiochem which contained 2.0 × 10⁻⁴ M NADH, 4.3 × 10⁻³ M fructose 1,6-bisphosphate, α-glycerolphosphate dehydrogenase, and triosephosphate isomerase buffered at pH 7.0. The activity was monitored by measuring the rate of loss of absorbance at 340 nm at 37 °C. Addition of **1** to an aldolase-assay mixture did not change the rate of decrease at 340 nm. The disappearance of absorbance at 340 nm was linear with time whether or

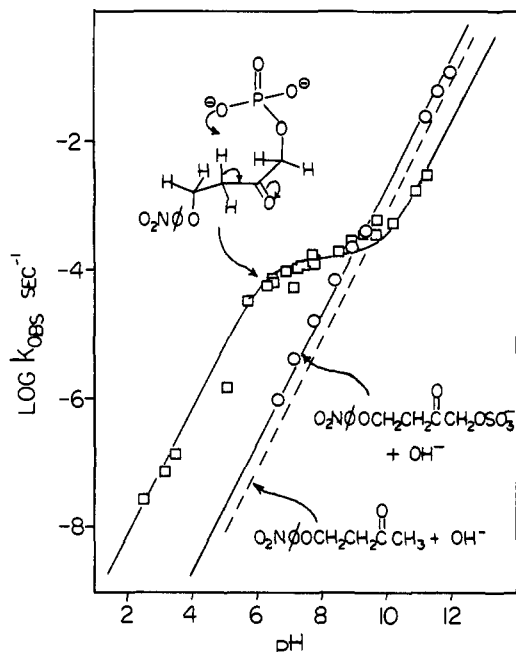
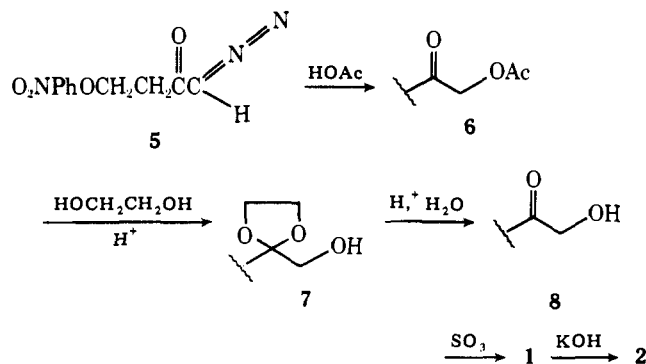


Figure 1. pH-rate profiles for the elimination of *p*-nitrophenol from **1** (○), from **3** (□), and from **9** (dashed line) are shown. The rate expression for **3** ($v = 1.30 \times 10^{-4} \text{ s}^{-1} [3^{2-}] + 2.13 \text{ M}^{-1} \text{ s}^{-1} [3^{2-}][\text{OH}^-]$) contains a term for the unimolecular decomposition of the dianion of **3** attributed to the intramolecular proton abstraction shown. The pH-rate profile for **1** ($v = 2.14 \times 10^1 \text{ M}^{-1} \text{ s}^{-1} [1^-][\text{OH}^-]$) has no such term and is similar to that found for **9** ($v = 8.1 \text{ M}^{-1} \text{ s}^{-1} [9][\text{OH}^-]$).

Scheme IV



not **1** was present in the assay mixture. All incubations and assays performed in this study were done at 37 °C.

Results

Compound **2** was synthesized from the previously described diazoketone **5** by the route shown in Scheme IV. The circuitous conversion of **5** to **8** proved to be much more efficient than more direct methods. Complete titration of the sulfate ester **1** with KOH invariably gave partial conversion to **2**, and, therefore, the last portion of the titration was carried out using the potassium salt of β -naphthoic acid. The β -naphthoic acid produced was filtered and extracted leaving pure $\text{K}^+ \text{1}^-$ behind. Appropriate NMR and UV spectra were obtained for **1** and **2** in a manner similar to that done previously for **3** and **4**.

The pH-rate profile for the conversion of **1** to **2** was measured by extrapolation of the rates in Tris solutions to zero buffer concentration. The results are shown in Figure 1 along with the pH-rate profile for **3** and that for 4-(4-nitrophenoxy)-2-butanone (**9**). The term found in the rate expression for **3** which was interpreted as evidence for intramolecular proton abstraction,⁶ as shown in Figure 1, was absent in the profile for **1**. The pH-rate profile for **1** is similar to that for **9**, which has no group available for intramolecular proton abstraction.

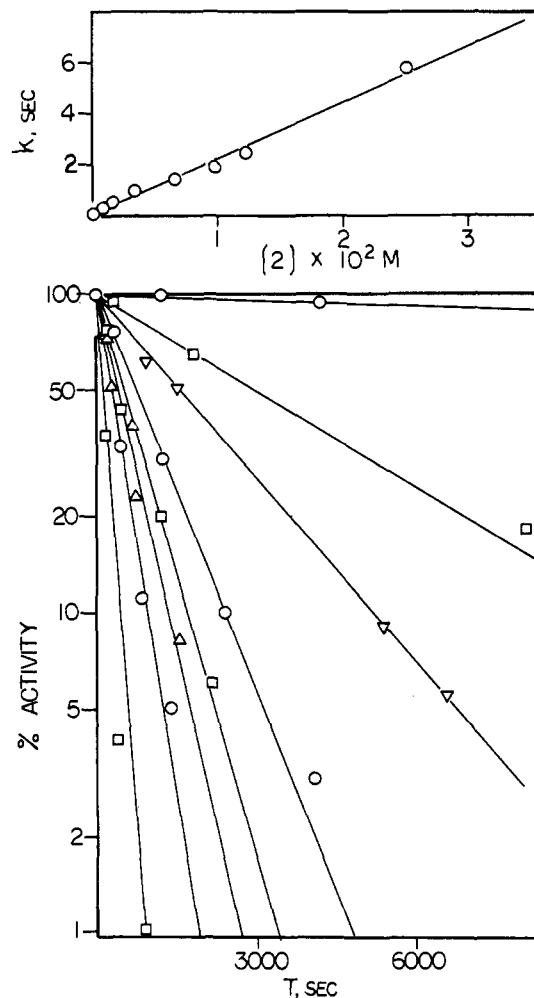


Figure 2. The lower plot shows the time-dependent loss of activity of aldolase in the presence of 0.00, 0.000 78, 0.001 56, 0.003 24, 0.006 48, 0.009 72, 0.0122, and 0.025 M **2**. The upper plot shows the linear dependence of k_{obsd} on $[2]$, which has a slope of $2.22 \times 10^{-1} \text{ s}^{-1} \text{ M}^{-1}$ which is equal to $k_{\text{obsd}}^{\text{max}}/K_i^1$.

As shown in Figure 2, incubation of **2** with aldolase does cause the time-dependent inactivation of the enzyme. The dependence of the rate constant for inactivation on the concentration of **2** is linear within the range studied. Higher concentrations of **2** would have altered the ionic strength substantially and created difficulty in the measurement of k_{obsd} because of the short half-time. Equation 1 describes the de-

$$\frac{1}{k_{\text{obsd}}} = \frac{K_i^1}{k_{\text{obsd}}^{\text{max}}[\text{I}]} + \frac{1}{k_{\text{obsd}}^{\text{max}}} \quad (1)$$

pendence of the rate on inhibitor concentration if the inhibitor binds reversibly (with a steady-state equilibrium constant for $\text{E} \cdots \text{I} \rightarrow \text{E} + \text{I}$ of K_i^1) and a maximum rate constant for the subsequent irreversible inactivation of $k_{\text{obsd}}^{\text{max}}$.^{6,10} The data in Figure 2 allow an accurate value of $2.22 \times 10^{-1} \text{ s}^{-1} \text{ M}^{-1} = k_{\text{obsd}}^{\text{max}}/K_i^1$ to be determined, where $\text{I} = \text{2}$. The data are not sufficient to determine both $k_{\text{obsd}}^{\text{max}}$ and K_i^1 , however.

Figure 3 shows the effect of adding the natural substrate DHAP to incubation mixtures containing **2**. DHAP protects against inhibition by **2**, as expected. Using eq 2^{6,10} and the

$$\frac{1}{k_{\text{obsd}}} = \frac{K_i^1}{k_{\text{obsd}}^{\text{max}}[\text{I}]} \left(1 + \frac{[\text{DHAP}]}{K_m^{\text{DHAP}}} \right) + \frac{1}{k_{\text{obsd}}^{\text{max}}} \quad (2)$$

known value of $k_{\text{obsd}}^{\text{max}}/K_i^1$, a value of K_m for DHAP of $6.9 \times 10^{-6} \text{ M}$ was computed. This value is similar to the value of $4.5 \times 10^{-6} \text{ M}$ reported by Rose,¹¹ and both of these values are larger than that measured by protection from inhibition by **4**.⁶

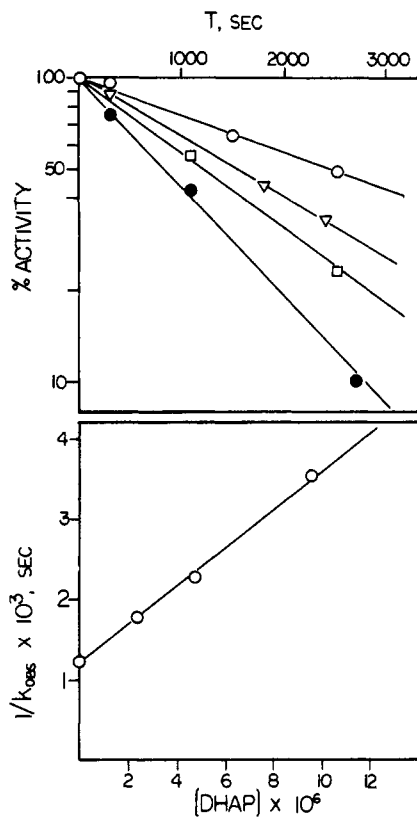


Figure 3. The upper plot shows the time-dependent inhibition of aldase in the presence of 2.78 ± 10^{-3} M **2** and 0 (●), 2.39×10^{-6} (□), 4.78×10^{-6} (▽), and 9.56×10^{-6} M DHAP (○) at pH 7.0. The lower plot shows the dependence of $1/k_{\text{obs}}$ on DHAP concentration which has a slope of $K_i^1/k_{\text{obs}}^{\text{max}}[1]K_m^{\text{DHAP}} = 2.34 \times 10^8$ s M⁻¹. Since $k_{\text{obs}}^{\text{max}}/K_i^1 = 2.22 \times 10^{-1}$ s⁻¹ M⁻¹, this gives a value of $K_m^{\text{DHAP}} = 6.9 \times 10^{-6}$ M.

The last value was measured at a very low ionic strength, however, and this is probably the source of the difference.

Discussion

The pH-rate profile shown in Figure 1 demonstrates the fact that an α -ketophosphate in the dianionic form catalyzes its own enolization with an effective molarity of 0.4 M.⁶ The corresponding reaction for an α -ketosulfate does not contribute to the overall rate at neutral pH. This is reasonable since the sulfate monoanion is a much weaker base ($\text{p}K_a(\text{ROSO}_3\text{H}) < 1$)¹² than the phosphate dianion ($\text{p}K_a(\text{ROPO}_3\text{H}^-) = 6.8$).⁶ An enzymatic reaction relying on an intramolecular proton transfer catalyzed by a phosphate dianion at neutral pH would be expected to fail with the analogous sulfate.

The enone sulfate **2** does act as an essentially irreversible inhibitor of aldase as did **4**, causing time-dependent loss of activity. As shown in Figure 2, there is a linear dependence upon **[2]** giving a value of $k_{\text{obs}}^{\text{max}}/K_i^2$ of 2.22×10^{-1} M⁻¹ s⁻¹. DHAP affords protection from inhibition by **2**, which indicates that **2** is acting as an active site directed inhibitor.

If the value of K_i^2 were known, the magnitude of $k_{\text{obs}}^{\text{max}}$ would also be fixed. It is possible to estimate this value if the equation $K_i^{\text{DHAS}}/K_m^{\text{DHAP}} = K_i^2/K_i^1$ holds. This presumes that changing from the phosphate to the sulfate group has about the same effect on the reversible binding of the inhibitors that it did on the binding of DHAS and DHAP. Figure 4 shows a plot of $1/k_{\text{obs}}$ for reduction of DHAS by 6.2×10^{-4} M sodium borohydride at pH 8.0 vs. DHAS concentration. The values of k_{obs} were computed from data obtained by Grazi⁵ and show that K_i^{DHAS} is $\sim 10^{-2}$ M. This suggests that $K_i^2 \approx 10^{-2} \times 10^{-4}/6 \times 10^{-6} \approx 0.2$ M. This value leads to $k_{\text{obs}}^{\text{max}} \approx 0.04$ s⁻¹ as the rate constant for conversion of the dissociable complex of aldolase and **2** to inhibited enzyme. The corresponding value

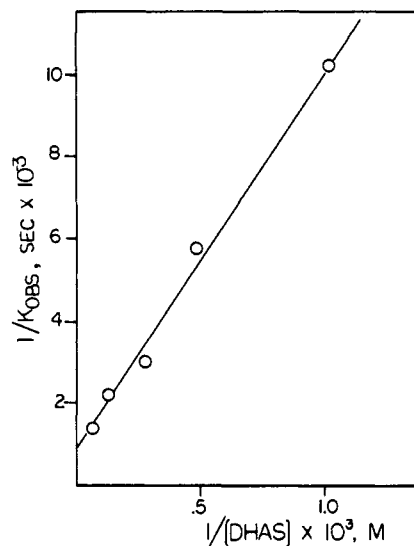


Figure 4. Values of $1/k_{\text{obs}}$ for reduction of aldolase-DHAS iminium ion by 6.2×10^{-4} M BH_4^- at pH 8.0 plotted vs. $1/[\text{DHAS}]$. The slope, $K_i^{\text{DHAS}}/k_{\text{obs}}^{\text{max}} = 9.12$ M⁻¹ s, and intercept, $1/k_{\text{obs}}^{\text{max}} = 900$ s, give a value of $K_i^{\text{DHAS}} = 1.01 \times 10^{-2}$ M. The data were taken from Grazi et al., ref 5.

for **4** was 0.112 s⁻¹. We conclude that though the change from phosphate to sulfate does substantially change the equilibrium constant for reversible binding of the covalent inhibitor, the rate at which the complex is converted to inactive enzyme is essentially unchanged. In terms of the mechanism proposed,⁶ this would mean that the rate of the attack of the cysteine thiol on the Michael acceptor was unchanged and, therefore, that the ability of the iminium ion to act as an electron sink was not substantially altered. All of these results are consistent with the intramolecular mechanism for proton abstraction.

It is an interesting fact that all aldolases operate by removing a proton and replacing it with the aldehyde on the same face¹³ of the intermediate enamine or enolate anion. This retention of configuration requires that the proton abstracting base swing out of the way so that it may be replaced by RCHO.¹⁴ We have proposed that the evolutionary pressure that invariably caused the selection of this particular stereochemically cryptic¹³ pathway arose because of the protection that this mechanism affords against enolization and subsequent racemization or dehydration of sugars.⁶ After the aldol condensation occurs, the proton abstracting base is automatically precluded from the site where proton abstraction may occur, and aldolases, therefore, are excellent catalysts for the enolization of trioses but are completely incapable of catalyzing the same reaction on six carbon sugars.

Presented in Figure 5 is a proposed mechanism for aldolase which integrates the intramolecular step for proton abstraction with the stereochemical requirements described above. The mechanism is consistent also with a variety of data concerning the order of addition of reactants and the presence of various functional groups at the active site. The protein cleft is approximated by the box drawn over the atoms which is open to solvent on the top and far side.

Rose has demonstrated by isotopic exchange at equilibrium¹⁵ that aldolase operates with an ordered mechanism whereby formation of an iminium ion with DHAP (a) is followed by loss of the *pro-S* proton¹⁶ at C-3 (b). The proton abstraction step occurs prior to the binding of G-3-P (c) which precedes formation of the iminium ion of F-1,6-P₂ (d). This iminium ion subsequently hydrolyzes to generate the keto form¹⁷ of F-1,6-P₂.

In step a, the conformation drawn is that consistent with the fact that only the *pro-S* proton on C-3 is exchanged with solvent.¹⁶ It has been drawn, therefore, facing the solvent and in

a position such that the *pro-S* C-H bond can overlap with the π orbital of the iminium ion during proton abstraction, as Spencer has shown to be extremely important.¹⁸ The face of the iminium ion exposed to solvent in Figure 5a has been shown by Grazi¹⁹ to be the side attacked by borohydride and, therefore, also presumably by water. The *E* isomer of the iminium ion has been drawn because this allows hydrogen bonding between the C-3 hydroxyl and the iminium ion. This would explain the fact that the iminium ion generated by the condensation of hydroxyacetone phosphate (with no OH on C-3) with the lysine amino group is less stable than that formed with DHAP.^{20,21} The C-1 phosphate has been drawn hydrogen bonded to an arginine residue that is known to be at the active site.²² This provides an iminium ion sufficiently exposed to solvent so that it may react with borohydride² or cyanide³ (or the subsequent enamine with tetranitromethane²³). Part of the bottom surface of the cleft is a cysteine thiol that is responsible for inactivation upon reaction with **2** and with **4**, with α -iodoacetol phosphate²⁴ and with carboxyethyl disulfide.²⁵

In step b the phosphate group is shown as having rotated to an alternate position where it may perform the intramolecular proton abstraction of the *pro-S* proton with the required overlap of the incipient p orbital with the iminium ion.¹⁸ The sulfate of DHAS would be too weakly basic for this task, whereas the phosphate dianion ($pK_a(\text{ROPO}_3\text{H}^-) = 6.8$) fits well with the prediction^{26,27} that the most effective proton abstractor will have a pK_a equal to the pH of the solution. We propose that the phosphate is positioned by a hydrogen-bonded combination of the imidazole group of His-359 and the phenol group of C-terminal Tyr-361.²⁸ Acetylation²⁹ or removal of Tyr-361 by treatment with carboxypeptidase causes a lowering of the rate of the proton transfer.¹⁵ In the F-1,6-P₂ cleavage direction, the enamine generated is protonated slowly to produce DHAP but still reacts rapidly with aldehydes so that the modified enzyme acts as a *trans*-aldolase. Photooxygenation of the imidazole groups decreases the rate of proton transfer³⁰ and increases the rate at which the tyrosine may be iodinated³¹ or acetylated.²⁹ Hartman has shown that His-359 is at the active site since it is attacked by an active site directed alkylating agent.³² This evidence suggests the intimate relationship between His-359, COOH-terminal Tyr-361, and the proton abstracting catalyst that is reflected in Figure 5b.

In step c, the acceptor aldehyde binds after the phosphate has lost a proton to solvent and then rotated back to its original position. Although there is considerable latitude possible in the structure of the aldehyde acceptor,¹ there must be a second phosphate binding site since cleavage of F-1,6-P₂ is much faster than cleavage of F-1-P.¹⁵ The aldehyde carbonyl must be protonated by a stereospecific catalyst rather than by water since tagatose 1,6-bisphosphate (which is identical with fructose 1,6-bisphosphate except for an inverted configuration at C-4) is not cleaved. This function and the C-6 phosphate binding could provide a role for the other lysine residues known to be at the active site.^{32,34}

In step d the iminium ion is formed and in a position to be attacked on the *re* face¹⁹ by water to form the carbinolamine which then can eliminate the lysineamine to generate the keto form¹⁷ of the F-1,6-P₂. It is clear from the geometry of F-1,6-P₂ that the C-3 proton is protected from enolization by the underside surface of the cleft and by the fact that the only bond capable of overlap with the iminium ion is a C-C bond. The only base able to perform an α -proton abstraction is automatically prevented from accomplishing this task because of the retention mechanism selected by evolution. It is clearly reasonable that compound **3** should bind to this active site with a favorable equilibrium constant suggesting iminium ion formation but be unable to undergo proton abstraction or subsequent elimination of *p*-nitrophenoxide, as has been found.⁶

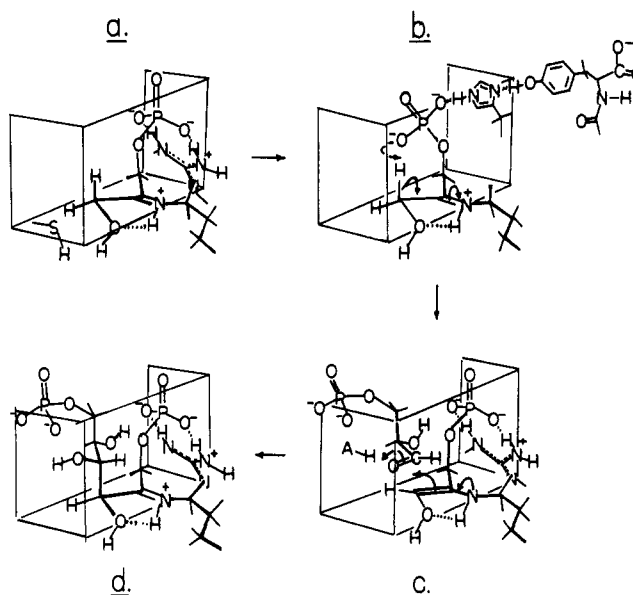


Figure 5. A proposed mechanism for aldolase, as described in the text, which incorporates the intramolecular proton transfer and which is consistent with other stereochemical and mechanistic features of the enzyme.

Acknowledgments. This work was supported in part by the American Cancer Society through an institutional grant.

References and Notes

- Horecker, B. L.; Tsolas, O.; Lal, C. Y. *Enzymes*, 3rd Ed. **1972**, 7, 213.
- Grazi, E.; Cheng, T.; Horecker, B. L. *Biochem. Biophys. Res. Commun.* **1962**, 7, 250.
- Cash, D. J.; Willson, I. B. *J. Biol. Chem.* **1966**, 241, 4290.
- Rose, I. A.; Rieder, S. V. *J. Biol. Chem.* **1956**, 231, 315.
- Grazi, E.; Sivieri-Pecorari, C.; Gagliano, R.; Trombetta, G. *Biochemistry* **1973**, 12, 2583.
- Motlu-DeGroot, R.; Hunt, W.; Wilde, J.; Hupe, D. J. *J. Am. Chem. Soc.* **1979**, 101, 2182.
- Wilde, J.; Hunt, W.; Hupe, D. J. *J. Am. Chem. Soc.* **1977**, 99, 3319.
- Budzikiewicz, H.; Djerassi, C.; Williams, D. "Mass Spectrometry of Organic Compounds"; Holden-Day: San Francisco, 1967; p 262.
- Donovan, J. W. *Biochemistry* **1964**, 3, 67.
- Meloche, H. P. *Biochemistry* **1967**, 6, 2273.
- Rose, I. A.; O'Connell, E. L. *J. Biol. Chem.* **1969**, 244, 126.
- Brownstein, S.; Stillman, A. E. *J. Phys. Chem.* **1959**, 63, 2061.
- Hanson, K. R.; Rose, I. A. *Acc. Chem. Res.* **1975**, 8, 1.
- Meloche, H. P.; Glusker, J. P. *Science* **1973**, 181, 350.
- Rose, I. A.; O'Connell, E. L.; Mehler, A. H. *J. Biol. Chem.* **1965**, 240, 1758.
- Rieder, S. V.; Rose, I. A. *J. Biol. Chem.* **1959**, 234, 1007.
- Midefort, C. F.; Gupta, R. K.; Rose, I. A. *Biochemistry* **1976**, 15, 2178.
- Ferran, Jr., H. E.; Roberts, R. D.; Jacob, J. N.; Spencer, T. A. *J. Chem. Soc., Chem. Commun.* **1976**, 49.
- Dilasio, A.; Trombetta, G.; Grazi, E. *FEBS Lett.* **1977**, 73, 244.
- Rose, I. A.; O'Connell, E. L. *J. Biol. Chem.* **1969**, 244, 126.
- Pratt, R. F. *Biochemistry* **1977**, 16, 3988.
- Lobb, R. R.; Stokes, A. M.; Hill, H. A. O.; Riordan, J. F. *Eur. J. Biochem.* **1976**, 70, 517.
- Healy, M. J.; Christen, P. *J. Am. Chem. Soc.* **1972**, 94, 7911.
- Hartman, F. C. *Biochemistry* **1970**, 9, 1783.
- Kowal, J.; Cremona, T.; Horecker, B. L. *J. Biol. Chem.* **1965**, 240, 2485.
- Hupe, D. J.; Kendall, M. C. R.; Spencer, T. A. *J. Am. Chem. Soc.* **1972**, 94, 1254.
- Hupe, D. J.; Kendall, M. C. R.; Spencer, T. A. *J. Am. Chem. Soc.* **1973**, 95, 2271.
- Lal, C. Y.; Nakal, N.; Chang, D. *Science* **1974**, 183, 1204.
- Pugh, E.; Horecker, B. L. *Arch. Biochem. Biophys.* **1967**, 122, 196.
- Hoffee, P.; Lal, C. Y.; Pugh, E. L.; Horecker, B. L. *Proc. Natl. Acad. Sci. U.S.A.* **1967**, 57, 107.
- Pugh, E.; Horecker, B. L. *Biochem. Biophys. Res. Commun.* **1967**, 26, 360.
- Hartman, F. C.; Welch, M. H. *Biochem. Biophys. Res. Commun.* **1974**, 57, 85.
- Tung, T. C.; Ling, K. H.; Byrne, W. L.; Lardy, H. A. *Biochim. Biophys. Acta* **1954**, 14, 488.
- Hartman, F. C.; Brown, J. P. *J. Biol. Chem.* **1976**, 251, 3057.